Korean J. Chem. Eng., **22**(5), 697-704 (2005)

Numerical Simulation of the Effects of the Design Feature of a Cyclone and the Inlet Flow Velocity on the Separation of CO_2 Particles from a CO_2-COF_2 Mixture

Younggeun Park, Chang Yeon Yun*, Jongheop Yi* and Honggon Kim,†**

Samsung Electro Mechanics, #314 Maetan-3-dong, YeongTong-gu, Suwon City, Gyeonggi 442-743, Korea
*School of Chemical Engineering, Institute of Chemical Processes,
Seoul National University, Shillim-dong, Kwanak-gu, Seoul 151-742, Korea
**Reaction Media Research Center, Korea Institute of Science and Technology,
39-1 Hawolgokdong, Seoul 136-791, Korea
(*Received 6 December 2004 • accepted 25 May 2005*)

Abstract–In synthesizing COF_2 from CO, a considerable amount of CO_2 is produced. A method of solidifying CO_2 at low temperature and separating CO_2 particles from the COF_2 gas using a cyclone was designed and the separation efficiency according to the cyclone feature was studied. Optimal sizing and operation conditions of the cyclone were investigated by reviewing the flow velocity profile and the particle trajectory using a numerical analysis with computational fluid dynamics (CFD). The effects of the inlet flow velocity and the ratio of the cyclone diameter to the cone length (D/L) on the recovery efficiency were estimated. Results revealed that the separation efficiency increases with an increase in the ratio of D/L and a decrease in the cyclone size. The recovery efficiency of CO_2 increases with the increase in the inlet flow velocity. Based on these results, we could propose a concept and methodology to design the optimal features and sizing of a cyclone suitable for separating solid CO_2 from gaseous COF_2 at low temperature.

Key words: Cyclone, Computational Fluid Dynamics (CFD), Two-Phase Simulation, Separation

INTRODUCTION

COF_2 is a potential alternative gas to be used in a CVD chamber as a dry cleaning agent in manufacturing semiconductors and LCDs because it contains fluorine like C_2F_6, C_3F_8 and NF_3. Several preparative methods for COF_2 have been reported: the halogen exchange reaction of $COCl_2$ with HF or alkali metallic fluorides dispersed in aqueous HF [Franz, 1979], the disproportionation of COClF over an active carbon catalyst [Ashton and Ryan, 1987], the oxidation of $CHClF_2$ in a Ni tube at elevated temperatures [Bay and Coates, 1988], the reaction of CO with fluorine-containing compounds such as SiF_4 or CaF_2 in an excited state produced by a plasma torch [Webster, 1996], the catalytic decomposition of oxyfluoro compounds such as $CF_3O(CF_2O)_n$-R over metal fluorides [Irie, 2003], the direct fluorination of CO_2 [Takashima and Yonezawa, 2003] and CO [Mori et al., 2003] with diluted F_2 gas, the fluorination of CO with metallic fluorinating agents such as CoF_3, CeF_4, AgF_2 and K_3NiF_3 [Mori and Ohashi, 2003]. Even in the most plausible methods for scale-up where COF_2 is synthesized from CO by using a considerable amount of fluorinating agent such as CoF_3 or AgF_2, CO_2 is commonly produced as a by-product. It is very costly to separate COF_2 and CO_2 using the conventional distillation method because their boiling points are close to each other. A method for solidifying CO_2 at low temperature and separating the CO_2 particles from COF_2 gas can be an alternative method for separating CO_2 from COF_2. A method of screening particles of CO_2 out by flowing the CO_2-COF_2 mixture through a fine screen or a membrane is one way to separate solid CO_2 from gaseous COF_2. However, openings of the screen or pores in the membrane become blocked by the screened CO_2 particles that are stacked on the separating medium surface, causing the flow of COF_2 through the medium to quickly decay. In this case, a cyclone seems to be a good method to separate CO_2 particles from COF_2 gas without having to risk any decrease in the separation efficiency or separation time because no separating medium is required.

The cyclone is known to be a useful gas-solid separator because of its simple design and the low operating cost. It is extensively applied in the environmental and chemical industries [Mariana et al., 2004]. It can also be used for heavily loaded gases or under severe conditions such as high temperature and high pressure. In a cyclone, a mixture of gas and solid enters the cylindrical or conical chamber tangentially through the duct-type inlet and the gas leaves through an opening on the top of the central axis. The solid particles move toward the separator wall by the inertial force and slowly settle down into the outlet at the bottom according to the decreasing circulation velocity. In other words, the gas-solid mixture becomes separated by the centrifugal acceleration. The centrifugal separating force or acceleration may range from 5 times the gravitational force in low-resistance cyclones with large diameters to 2,500 times the gravitational force in high-resistance units with very small diameters [Perry et al., 1984].

The cyclone also has disadvantages. It shows a low separation efficiency rate when collecting particles with a diameter smaller than 1 μm. In general, cyclones are designed to satisfy the specific pressure-drop. In the ordinary cyclone system operated at a near atmospheric pressure, the fan is designed to be suitable for the maximum allowable pressure drops corresponding to the inlet flow velocities ranging from 6 to 21 m/sec. They are often designed for the inlet flow velocity of about 15 m/sec. The reduction of the gas-outlet duct diameter increases both the separation efficiency and the pressure drop. Although there are not many reliable data, it is a

†To whom correspondence should be addressed.
E-mail: hkim@kist.re.kr

known trend that the increase of the cyclone length leads to higher separation efficiency, and the increase of the gas inlet velocity increases the collection efficiency. However, when the solids are apt to agglomerate inside, the increased velocity tends to most likely cause deflocculation in the cyclone, which in turn causes the efficiency to remain the same or to decrease. It is obvious that the turbulence brings about the agglomeration effect because the intensity of the turbulence is very strong.

When the particle concentration is high, the separation efficiency generally decreases with the increase in the particle concentration [Hoffmann, 1991; Fayed and Otten, 1984; Xiaodong et al., 2003]. Tuzla and Chen [1992] reported that there is an optimal particle concentration where the separation efficiency is the highest. Bloor and Iagham [1983] also showed that the separation efficiency increases with the increase in the tangential velocity at high particle concentration. However, they only investigated the influence of the particle phase on the mean flow fields and did not study the turbulence structure. Peskin [1982] studied the interaction of the gas phase and the solid phase in the turbulence and found that the particles with a small diameter (<0.5 mm) can weaken turbulent fluctuations in the gas phase. They reported that the primary design factor to be considered for controlling the separation efficiency is the cyclone diameter. It was found that a cyclone with a smaller diameter shows a higher flow velocity and a higher fractional collection efficiency. Small-diameter cyclones, however, should be used in a bundle of multiple units in parallel in order to satisfy a specified capacity. It has also been reported that there are other geometrical design factors, such as the body length and the outlet diameter, that also have certain effects on the efficiency [Perry et al., 1984]. Yoshida and Yang [1991] reported that the particle separation efficiency is strongly dependent on the mist injection.

While reviewing the previous results, we found that the effect of the inlet velocity and the ratio of the cyclone radius to the cone length on the separation efficiency have not been yet estimated for severe conditions such as low temperature. In addition, the optimal operating condition in a small-scale cyclone is not clear. Thus, in this work, a model of three-dimensional computational fluid dynamics (CFD) was used to calculate the flow patterns and the particle trajectory. In addition, the effect of the inlet velocity and the ratio between the cyclone radius and the cone length were estimated for different designs and conditions at low temperature. Finally, based on the experimental results, we propose herein the optimal design factor and operating conditions for separating the solid CO_2 particles from the CO_2-COF_2 mixture through the solidification of CO_2 at low temperature.

UNDERLYING THEORY

1. Critical Particle Diameter, CPD

Even though there have been various efforts to theoretically predict the cyclone performance, a clear relationship has not yet been found. Some attempts have been made to predict the critical particle diameter (CPD), which will be the theoretical size of the smallest particle separable from the gas stream. This approach embodies various assumptions concerning the gas-flow pattern and the path of a particle in the cyclone. In a study, Rosin, Rammler and Intelmann assumed that the gas stream undergoes a fixed number of turns at a constant spiral velocity equal to the average velocity in the cyclone inlet without any turbulence or mixing action, and that Stoke's law holds for the motion of a particle in the centrifugal field [Perry et al., 1984]. Other researchers such as Barth and Brennst made similar derivations but used different assumptions concerning the flow pattern. The most popular empirical expression of CPD proposed by Rosin, Rammler and Intelman for a reverse-flow type cyclone is adopted [Perry et al., 1984].

$$D_{p,min}=\left[\frac{9\mu B_c}{\pi N_{tc} V_c(\rho_p-\rho)}\right]^{0.5} \tag{1}$$

where $D_{p,min}$ is identical with CPD, N_{tc} is the number of turns made by the gas stream in a cyclone, ρ_p is the particle density, ρ is the gas density, B_c is the width of the inlet duct, V_c is the average inlet velocity of fluid, and μ is the gas viscosity.

2. Governing Equation

The flow patterns are calculated by means of three-dimensional equations based on the Navier-Stokes equations of the total continuity, energy and momentum. A steady state is assumed for the system.

$$\frac{\partial}{\partial x_i}(\rho u_i)=0 \tag{2}$$

$$\frac{\partial}{\partial x_i}(\rho u_i h)=\frac{\partial}{\partial x_i}(k+k_t)\frac{\partial T}{\partial x_i}-\frac{\partial}{\partial x_i}\sum_j h_j J_j+\frac{\partial p}{\partial x_i}+\tau_{ij}\frac{\partial u_i}{\partial x_j}+S_h \tag{3}$$

$$\frac{\partial}{\partial x_i}(\rho u_i u_j)=-\frac{\partial P}{\partial x_i}+\frac{\partial \tau_{ij}}{\partial x_j}+\rho g_i+F_i \tag{4}$$

where T is the temperature of the mixture flow, ρ is the flue gas density, P is the pressure, τ_{ij} is the viscous stress tensor, J_j is the flux of species j, u_i is the fluid velocity for i direction, g_i is the gravitational acceleration, k is the thermal conductivity of the mixture, k_t is the thermal conductivity of turbulence flow, F_i is the external body force in the i direction, h is the enthalpy of mixture, h_j is the enthalpy of the species j, and S_h is a term that includes sources of enthalpy due to chemical reactions, radiations, and heat exchanges with the dispersed second phase.

The standard k-ε turbulence model is adopted to estimate the turbulence phenomena in a cyclone.

$$\frac{\partial}{\partial x_i}(\rho u_i \kappa)=\frac{\partial}{\partial x_i}\frac{\mu_t}{\sigma_\kappa}\frac{\partial P}{\partial x_i}+G_\kappa+G_b-\rho\varepsilon \tag{5-1}$$

$$\frac{\partial}{\partial x_i}(\rho u_i \varepsilon)=\frac{\partial}{\partial x_i}\frac{\mu_t}{\sigma_\varepsilon}\frac{\partial P}{\partial x_i}+C_{1\varepsilon}\frac{\varepsilon}{\kappa}(G_\kappa+(1-C_{3\varepsilon})G_b)-C_{2\varepsilon}\rho\frac{\varepsilon^2}{\kappa} \tag{5-2}$$

κ, the turbulent kinetic energy, and ε, the dissipation rate of κ, are taken into consideration to estimate the flow velocity and the length scale. μ_t represents the turbulent viscosity, and $C_{1\varepsilon}$, $C_{2\varepsilon}$, $C_{3\varepsilon}$ are empirical constants. σ_κ and σ_ε are Prandtl numbers which consider the diffusion by κ and ε in turbulence [Yang and Yoshida, 2004; Launder and Spalding, 1972].

$$G_k=\mu_k\left(\frac{\partial u_j}{\partial x_i}+\frac{\partial u_i}{\partial x_j}\right)\frac{\partial u_j}{\partial x_i} \tag{6}$$

G_k is the rate of production of the turbulent kinetic energy.

$$G_b=-g_i\frac{\mu_t}{\rho\sigma_h}\frac{\partial \rho}{\partial x_i} \tag{7}$$

G_b is the generation of turbulence due to the buoyancy force [Laun-

der and Spalding, 1972].

3. Discrete Phase Model, DPM

The trajectory of a particle is estimated by the discrete phase model (DPM). The DPM integrates the force balance on the particle, which is written from a Lagrangian point of view.

$$\frac{du_p}{dt} = F_D(u - u_p) + \frac{g \cdot x(\rho_p - \rho)}{\rho_p} + F_x \quad (8)$$

$F_D(u-u_p)$ is the drag force per unit particle mass, and F_x is the external force. A relative velocity concept is applied in the DPM.

$$F_D = \frac{18\mu C_D Re}{\rho_p d_p^2 \ 24} \quad (9)$$

u is the fluid phase velocity, u_p is the particle velocity, μ is the molecular viscosity of the fluid, ρ is the fluid density, ρ_p is the particle density, and d_p is the particle diameter. Re is the relative Reynolds number which is defined as follows.

$$Re \equiv \frac{\rho d_p |u_p - u|}{\mu} \quad (10)$$

The drag coefficient, C_D, can be obtained from the following equation.

$$C_D = \alpha_1 + \frac{\alpha_2}{Re} + \frac{\alpha_3}{Re^2} \quad (11)$$

where a_1, a_2, and a_3 are constants that apply for smooth spherical particles for several ranges of Re given by Morsi and Alexander [Morsi and Alexander, 1972].

NUMERICAL ANLYSIS

This process was designed for separating CO_2 particles from the CO_2-COF_2 mixture at low temperature (about 215 K). In this simulation, the solidification of CO_2 and the particle size of solid CO_2 were key factors for the embodiment of a real process. In order to obtain accurate results, it is important to choose a suitable size of a CO_2 particle, because the size and the density of a particle are the driving forces in the cyclone separation.

Solidification of CO_2 (desublimation) is the direct conversion of CO_2 from vapor state to solid state without passing through the liquid state. Desublimation is widely used to purify chemicals since the resulting particles can be obtained in high purity and in good appearance. This concept was applied to separate CO_2 from the mixture with gaseous COF_2. Solid CO_2 has a vapor pressure of 1 atm at 194.6 K and a density approximately 1.5 times that of liquid CO_2 while the vapor pressure of CO_2 is 5.11 atm at its triple point, 216.8 K. The nucleation and growth of the particles depend on the spatial fields of temperature and concentration of CO_2 within the mixture. In order to get precise information about the particle growth, these fields should be experimentally measured. Since the gaseous CO_2 is presumed desublimated at low temperature before entering the cyclone inlet, the exact distribution of particle size cannot be easily obtained [Modde and Mewes, 1995]. Also, when the cooling time and the rate are increased, particles larger than 100 μm are readily collectible by simple inertial or gravitational methods according to the Ostwald ripening mechanism. However, the formation of CO_2 particles larger than 100 μm is inefficient from the point of cost.

Table 1. Profiles of injection particles

Name	Particle diameter [m]	Number of particles	Material
0	1×10^{-6}	10	COF_2
1	5×10^{-6}	10	COF_2
2	7×10^{-6}	10	CO_2
3	1×10^{-5}	10	CO_2
4	3×10^{-5}	10	CO_2
5	5×10^{-6}	10	CO_2
6	7×10^{-5}	10	CO_2
7	1×10^{-4}	10	CO_2

Table 2. Boundary conditions

		Temperature [K]	Normal inlet vel. [m/sec]
Inlet	Velocity inlet	215	12.5[a]/25.0[b]
Outlet 1	Upside outlet	215	-
Outlet 2	Downside outlet	215	-
Wall	-	Adiabatic	-

[a]normal inlet velocity of case I.
[b]normal inlet velocity of case II

Because this work focused on the effect of particle size in the separation of particles smaller than 100 μm, the separation efficiency and the characteristics were estimated in a distribution of particle sizes ranging from 1 μm to 100 μm and the same number of particles was assumed in each size of particle as shown in Table 1. The inlet duct temperature was fixed at 215 K, which is the middle point between the triple point of CO_2 (217 K at 5.11 atm) and the boiling point of COF_2 (210 K at 5 atm). At this low temperature, CO_2 is in a solid state while COF_2 is in a gaseous state. According to the literature [Perry et al., 1984] which showed the actual particle diameter of CO_2 being bigger than 7 μm and based on a general trend where the particle size increases with the decrease of temperature, it was assumed that the particles smaller than 7 μm were composed of COF_2, whereas the relatively larger particles were composed of CO_2. In the computational analysis, 80 particles were inserted at the inlet duct of the cyclone. Boundary conditions which seemed proper for a real operation are listed in Table 2. The cyclone simulation was performed in a three-dimensional hybrid grid (Fig. 1) consisting of 14,840 and 44,840 cells using a commercial computational fluid dynamics (CFD) code, Fluent v. 6.0. The semi-implicit pressure linked equation (SIMPLE) algorithm was applied to solve the momentum equation. The calculation for each case took about 6 hr of running time on a Pentium IV 1.2 GHz.

RESULTS AND DISCUSSIONS

1. Effect of Inlet Flow Velocity

The separation efficiency can be regulated by controlling the space velocity in the cyclone, which is determined by the inlet velocity and the tuning number of the fluid inside the cyclone. The velocity profile as a function of inlet velocity is shown in Fig. 2. It can be seen that fast flow regions exist around the inlet and the outlet of the cyclone (the pale region), while slow flows appear in the inner

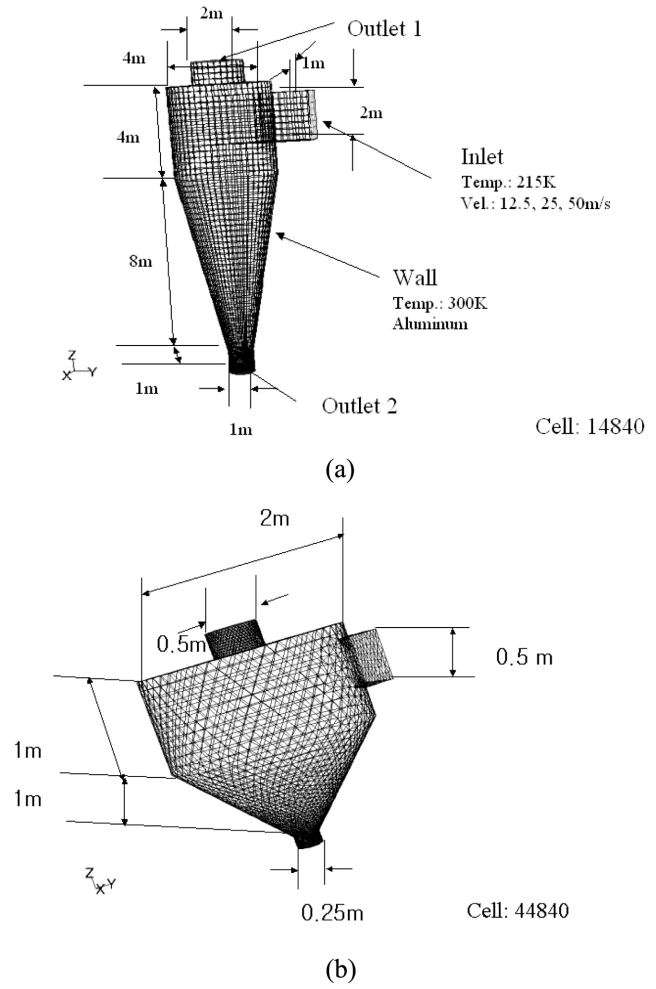

Fig. 1. Computational grid system: (a) typical cyclone and (b) modified cyclone system.

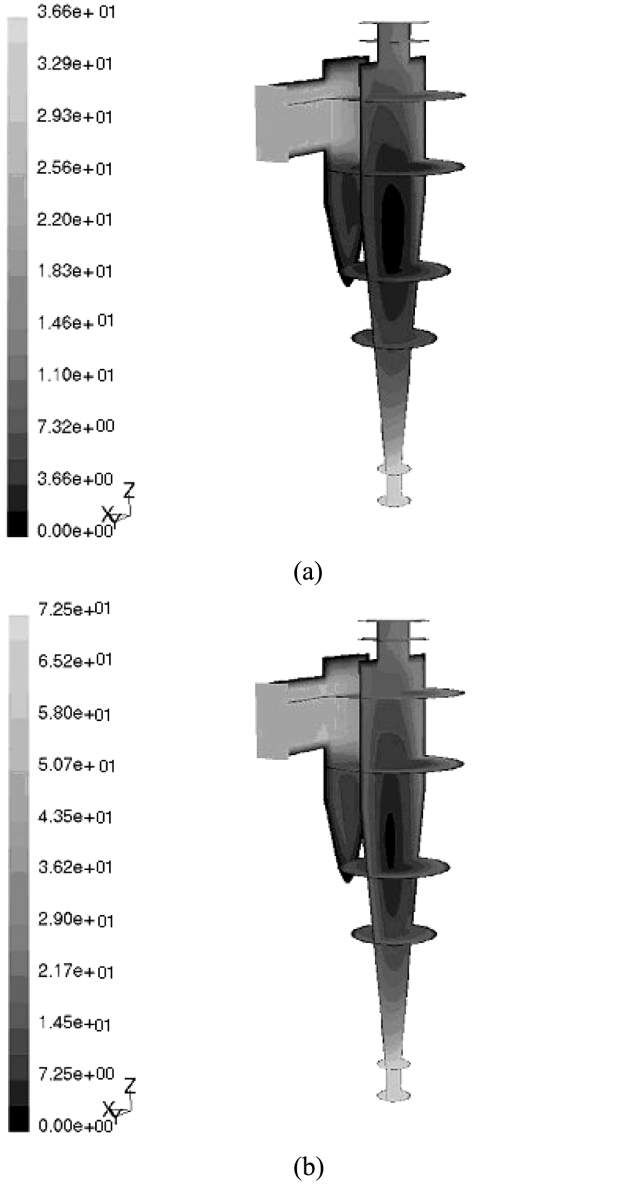

Fig. 2. Velocity magnitude profile as a function of inlet velocity: (a) vel.=12.5 m/s and (b) vel.=25 m/s.

part (the dark region). A circulating flow pattern of the particles inserted leads to the fast flow at the inner wall side. When the inlet velocity increases from 12.5 m/sec to 25 m/sec, the velocity profile increases as much as two times, but the highest velocity increases from 3.66 m/sec to 7.25 m/sec, which is a little lower than two times. The velocity difference between the inner and the wall side also increases with the increase in the inlet velocity, which is assumed to probably induce high separation efficiency.

The particle trajectory as a function of the inlet velocity in the cyclone of Design I is shown in Fig. 3. Due to the size limitation of Design I, controlling the particle size and the inlet velocity has no remarkable effect on the separation efficiency. Based on the particle size distribution at each outlet, an average particle size at the upside outlet is found to be 1 μm for 12.5 m/sec and 7 μm for 25 m/sec. A relatively slow inlet velocity has an advantage in separating small particles. Based on these facts, it can be deduced that the CO_2 particles of relatively large size are more likely to be separated at a high inlet flow velocity such as 50 m/sec.

2. Effect of Cyclone Design

In order to increase the turn number of particles in the cyclone, various modifications were made to the designs such as increasing the diameter of the cyclone, decreasing the cone length, etc. The relationship between the trajectory and the space-time in the cyclone of Design II is shown in Fig. 4. In Design I, the numbers of particles of 1mm emitted from the upside outlet and the downside outlet can be seen the same. The particles of 1mm inserted in the cyclone of Design II are, however, mostly emitted from the upside outlet. The space-time of the 1mm particle is 1.05×10 sec for Design I and 2.83×10 sec for Design II. The numbers of 5 μm particles emitted from the upside outlet and the downside outlet are the same even though the cyclone design changes. The weight portion of the particles at 1-5 μm is 0.084%.

The trajectories of solid particles as a function of cyclone diameter are also shown in Fig. 3 and Fig. 4. In Design I, the numbers of particles emitted from the upside outlet and the downside outlet are the same. Particles inserted in the cyclone of Design II are, however, emitted from the downside outlet regardless of the inlet velocity tested. The separation efficiency of Design I is zero without con-

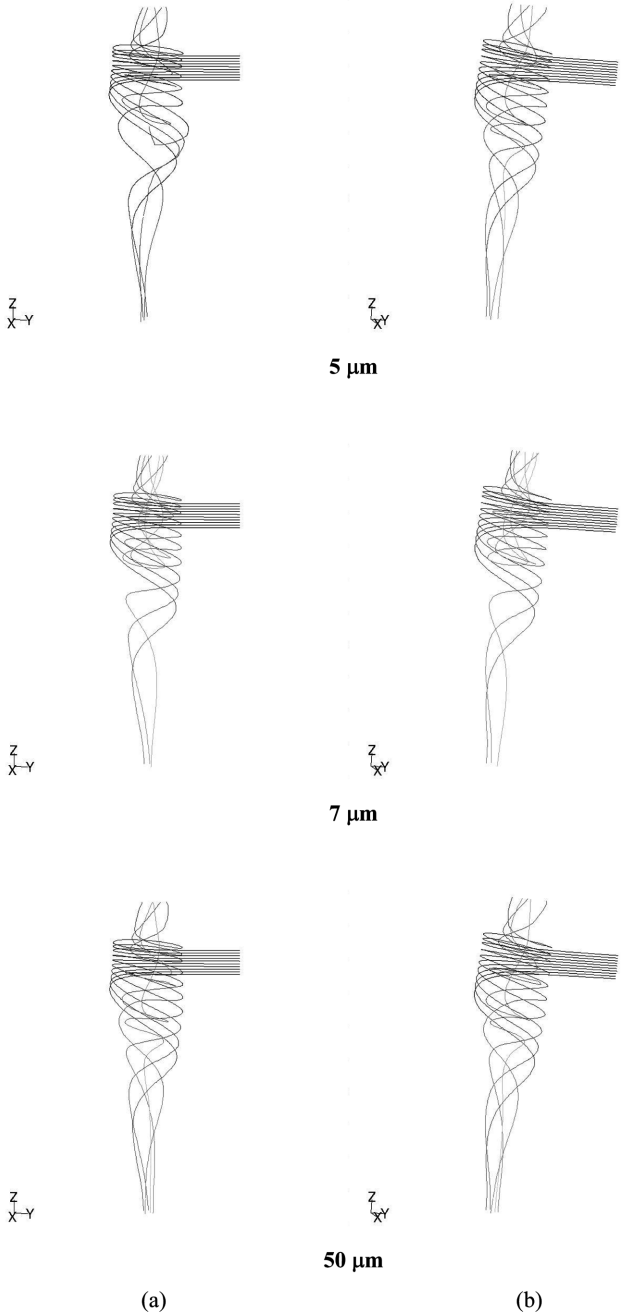

Fig. 3. Particle trajectory as a function of inlet velocity in Design I: (a) vel.=12.5 m/s and (b) vel.=25 m/s.

sideration of the particle size, but the separation characteristic of Design II is clearer than that of Design I. The separation efficiency as a function of the particle size increases with the ratio of the cyclone diameter to the cone length (Design I, D/L=1/3 →Design II, D/L=1). It was reported that five turns of particles leads to effective separation [Peskin, 1982]. Based on the simulation results, we found that about three turns are sufficient for separating particles in Design I regardless of the particle size. This pattern is probably induced by the reduction of the centrifugal force resulting from the decrease of the cyclone diameter, which is the most important factor in the cyclone design. In the case of Design II, when the inlet flow velocity at the cyclone duct increases, the turning number in the cyclone increases. The critical particle diameter (CPD), which is the minimum diameter for separating particles, is estimated by the simulation result for each cyclone (Table 3). Design II with 0.350 μm CPD shows higher separation capability, which indicates recovering more CO_2 particles from the mixture, than the Design I with 0.940 μm CPD. The effect of inlet flow velocity on CPD was observed. The CPD decreases with the increase in the turn number

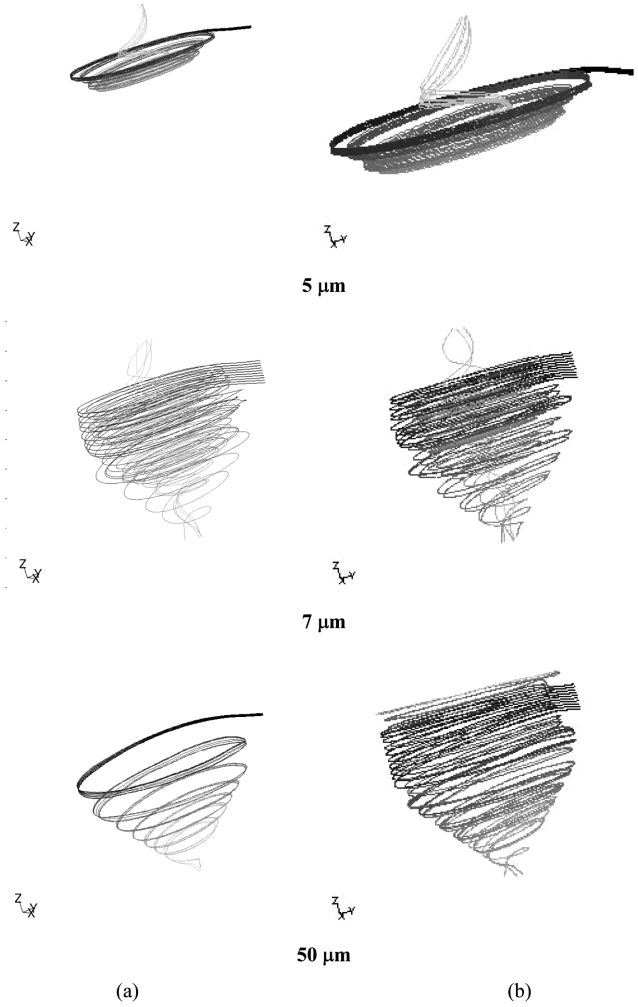

Fig. 4. Particle trajectory as a function of inlet velocity in Design II: (a) vel.=12.5 m/s and (b) vel.=25 m/s.

Table 3. Critical particle diameter of each cyclone

	Design I		Design II	
Estimated number of turns by simulation	3	3	5	5
Cyclone inlet velocity [m/sec]	12.5	25.0	12.5	25.0
Critical Particle Diameter [m]	9.04×10^{-7}	6.40×10^{-7}	3.50×10^{-7}	2.47×10^{-7}

of the cyclone. The insertion of large particles causes the particle turning region to move to a lower position. These results show that the cyclone diameter is a more decisive factor than the cone length for determining a proper turning number and a centrifugal force in the cyclone.

3. Effect of Scale-down

As mentioned above, the cyclone with a small diameter shows high turning velocity and high separation efficiency [Perry et al., 1984]. In order to test the applicability of a small-scale process or equipment, the scale of the proposed cyclone system was scaled down to 0.1 times of Design I and Design II (Design III; a small scale of Design I, Design IV: a small scale of Design II). In Fig. 5, the particle trajectory in the cyclone of Design III is shown as a function of the inlet flow velocity (1.25 m/sec and 2.5 m/sec). The growth of particle track is low in a small-scale cyclone. This pattern can be clearly seen in the case of a low inlet flow velocity. We cannot see any effect of particle size on the particle turning in a small-scale cyclone of Design III. When the inlet flow velocity increases, the separation efficiency and the turning number of small particles less than 10 μm increases as well, but there are no development of the particle trajectory and no improvement in the separation efficiency with large particles bigger than 10 μm. The space-time of particles in the cyclone of Design III is about 2-5 sec and similar to that in Design I or Design II. These values are probably because of the premature turbulence occurring as a result of the scale-down and not because of the flow developed inside the cyclone.

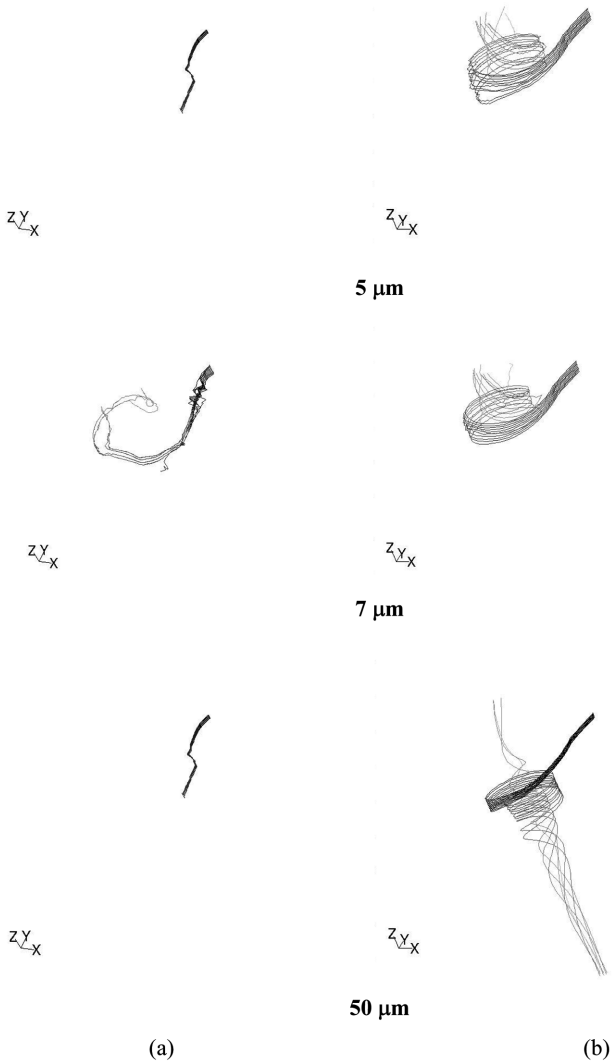

Fig. 5. Particle trajectory as a function of inlet velocity in Design III: (a) vel.=1.25 m/s and (b) vel.=2.5 m/s.

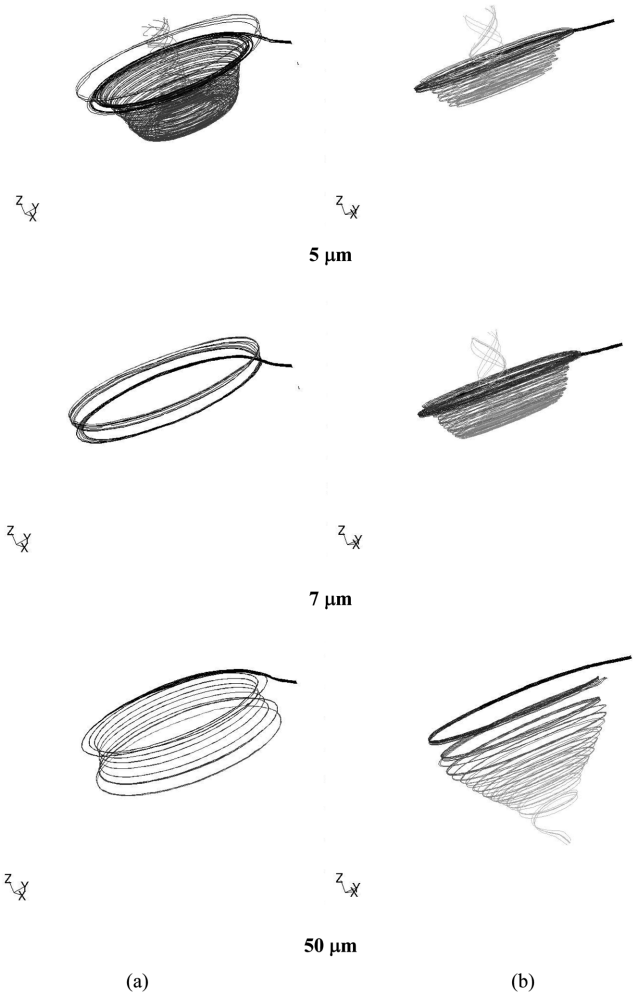

Fig. 6. Particle trajectory as a function of inlet velocity in Design IV; (a) vel.=1.25 m/s and (b) vel.=2.5 m/s.

In Fig. 6, the particle trajectories in the cyclone of Design IV are shown for the inlet flow velocities of 1.25 m/sec and 2.5 m/sec. The particle trajectory in the cyclone of Design IV shows a similar pattern in the cyclone of Design III. With a slow inlet flow velocity (1.25 m/sec), some particles of 5 μm (COF_2) were emitted from the upside outlet while no particles bigger than 5 μm (≥7 μm, CO_2) were emitted. A coiled trajectory of particles with the increased turning number (5 turns→10 turns) proposed a possible infinite flow circulation in this case. With a relatively fast inlet flow velocity (2.5 m/sec), particles of 5 μm (COF_2) and 7 μm (CO_2) were emitted from the upside outlet while bigger particles were emitted from the downside outlet. The turning number of CO_2 particles and the efficiency of recovering CO_2 can be seen to increase with the increase of the inlet flow velocity. One of the most plausible reasons for this pattern is the increase of the ratio of the cyclone diameter to the cone length, D/L.

4. Recovery Efficiency

We defined two kinds of CO_2 recovery efficiency in the cyclone: one is determined based on the weight of particles and the other is determined based on the number of particles. The CO_2 recovery efficiency based on the number of particles in the cyclone can be defined as follows.

$$\eta_n = \frac{\text{Output particle number to downside}}{\text{Input of total particle number}}$$

The CO_2 recovery efficiency based on the weight of particles in the cyclone can also be defined as follows.

$$\eta_W = \frac{\text{Output weight to downside}}{\text{Input of total particle weight}}$$

Fig. 7 shows the recovery efficiencies based on the weight, η_w, varying according to the design of cyclone. As mentioned before, the weight fraction of small particles emitted from the downside outlet is 0.084% which is almost negligible. From this figure, we can see that in the cyclones of Design II and IV, a η_w of 95% is achieved regardless of the various inlet flow velocities. The increase of the ratio D/L induces the increase of η_w by increasing the centrifugal force. In the same design shape of the cyclone, the η_w increases in the scale-downed cyclone system (Design I→Design III). In the case of a slow inlet flow velocity, a relatively high η_w of 95% is achieved in Design III, while no effect of the inlet flow velocity is observed in the cyclones of Design I, II and IV.

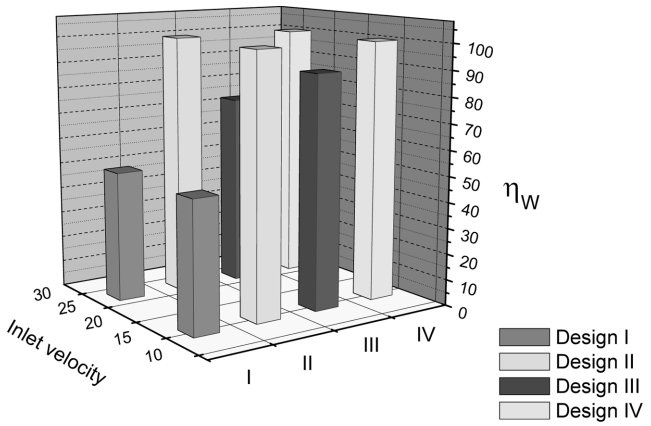

Fig. 7. Recovery efficiency of CO_2 particle based on weight of particles.

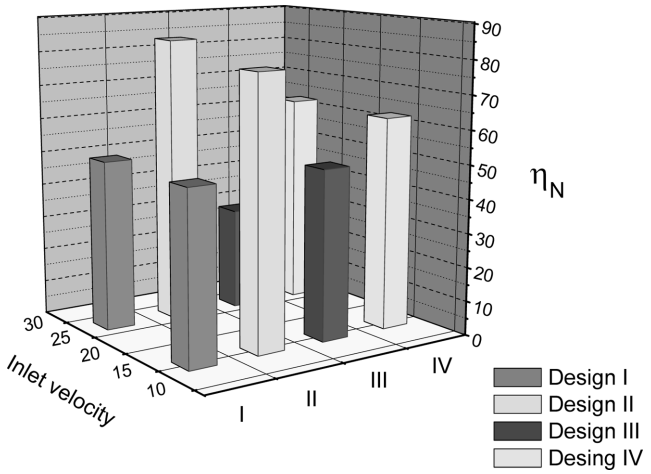

Fig. 8. Recovery efficiency of CO_2 particle based on number of particles.

Table 4. Particle size distribution at each outlet

Inlet vel. [m/s]	Mean particle size at upside outlet	Mean particle size at downside outlet
12.5	1×10^{-6} m	1×10^{-5} m
25.0	7×10^{-6} m	1.5×10^{-5} m

Fig. 8 shows the recovery efficiencies based on the particle number, η_n, varying according to the design of cyclone. Unlike the η_w, the η_n values are different according to the design and the inlet flow velocity. The values of η_w are in the following order: Design II> Design IV>Design I>Design III. This pattern shows that the centrifugal force in a cyclone of large D/L is an important factor to be considered in the CO_2 separation. In the case of η_n, a relatively high separation efficiency is also achieved at a slow inlet flow velocity in Design III.

CONCLUSIONS

We have shown the concept and methodology that CO_2 is separable from the CO_2-COF_2 mixture using a cyclone, and the cyclone with high separation efficiency can be designed via a numerical simulation. The velocity profile, the particle trajectory and the separation efficiency of cyclone were estimated and analyzed from the point of cyclone design for the separation of CO_2 from a CO_2-COF_2 mixture. Based on the results of the CFD simulation, we could make the following conclusions.

First, high separation efficiency can be achieved by increasing the ratio of the cyclone diameter to the cone length (D/L) if the body is long. Second, in order to separate CO_2 particles in the cyclone at low temperature, a fast flow of 25 m/sec is recommended, even though it was reported in previous literatures that a flow of about 15 m/sec is suitable for general cyclones. Third, when the scale of cyclone decreases, the external force such as the gravitational force has more influence than the inner centrifugal force. This effect can be overcome by increasing the ratio of the cyclone diameter to the cone length. Finally, when the inlet flow rate is slower than 12.5 m/s, the particles bigger than 7 μm (≥10 μm) cannot be emitted from the upside outlet, whereas particles smaller than 7 μm are emitted as much as 0.084% from the downside outlet. This result shows that the cyclone separation at low temperature can be applied for separating CO_2 and COF_2 with high efficiency of over 99.9% COF_2. Based on the foregoing, we propose optimal design conditions for cyclones with which the solid particles of CO_2, dry ice, can be separated from the CO_2-COF_2 mixture at a low temperature range.

ACKNOWLEDGMENT

This work was co-supported by the National Research Laboratory (NRL) of the Korean Science and Engineering Foundation (KOSEF) and the Grant of the Korea Institute of Science and Technology

(KIST).

NOMENCLATURE

B_c : width of rectangle cyclone inlet duct [m]
C_D : drag coefficient
d_p : particle diameter [m]
F_i : external force for i direction [N/m^2]
g : gravity acceleration [m/sec^2]
h : enthalpy of mixture [J/mol]
h_j : enthalpy of species j [J/mol]
j : component
J_j : flux of j [kg/m^2-sec]
k : thermal conductivity [W/m-K]
k_t : thermal conductivity of turbulent flow [W/m-K]
N_{tc} : number of turns made by gas stream in cyclone
P : pressure [Pa]
q : gas flow rate [m^3/sec]
S_h : external heat source by chemical reaction [W]
T : temperature [K]
u : fluid velocity [m/sec]
u_i : fluid velocity in i direction [m/sec]
u_p : particle velocity [m/sec]
V : average cyclone inlet velocity [m/sec]
x_i : distance in i direction

Greek Letters

ε : dissipation rate of κ [m^2/sec]
ρ_p : particle density [kg/m^3]
ρ : gas density [kg/m^3]
κ : turbulent kinetic energy [J/kg]
σ_h : turbulent Prandtl number
σ_κ : Prandtl number governing the turbulent diffusion of κ
σ_ε : Prandtl number governing the turbulent diffusion of ε
τ : shear stress for wall [Pa]
μ : fluid viscosity [Pa-sec]
μ_t : turbulent viscosity [Pa-sec]

REFERENCES

Ashton, D. P. and Ryan, T. A., *Method for the Preparation of Carbonyl Difluoride*, European Patent 253,527 (1987); *Carbonyl Difluoride Preparation*, U.S. Patent 5,241,115 (1993).

Bay, E. and Coates, M., *Production of Carbonyl Difluoride*, European Patent 310,255 (1988).

Bloor, M. L. G. and Iagham, D. B., *Theoretical Aspects of Hydrocyclone Flow, in: R. J. Wakeman (Ed.), Progress in Filtration and Separation Part III*, Elsevier, Amsterdam (1983).

Fayed, M. E. and Otten, L., *Handbook of Powder Science and Technology*, Van Nostrand Reinhold Co., New York (1984).

Franz, R., *Verfahren zur Herstellung von Carbonyl Difluoriden*, German Patent DE 2823981 (1979).

Henkes, R. A. W. M., van der Flugt, F. F. and Hoogendoorn, C. J., "Natural Convection Flow in a Square Cavity Calculated with Low-Reynolds-Number Turbulence Models," *Int. J. Heat Mass Transfer*, **34**, 1543 (1991).

Hoffmann, A. C., "An Experimental Investigation Elucidating the Nature of the Effect of Solids Loading on Cyclone Performance," *Filter. Sep.*, **28**, 188 (1991).

Irie, M., *Method for Producing COF_2*, Japan Patent 313,016 (2003).

Launder, B. E. and Spalding, D. B., *Lectures in Mathematical Models of Turbulence*, Academic Press, London, England (1972).

Mariana, S. K., Satake, T., Maezawa, A., Takeshita, T. and Uchida, S., "Experimental and Modeling Study on CO_2 Absorption in a Cyclone Scrubber by Phenomenological Model and Neural Networks," *Korean J. Chem. Eng.*, **21**, 589 (2004).

Modde, M. and Mewes, D., "Generation of Very Fine Solid Particles by Vapour Desublimation in a Gaseous Mixture," *J. Aerosol Sci.*, **26**(1), S565 (1995).

Mori, I. and Ohashi, M., *Method for Manufacturing Carbonyl Difluoride*, Japan Patent 146,620 (2003); Japan Patent 221,214 (2003).

Mori, I., Tomura, T., Kondo, T., Ohashi, M. and Kanashima, T., *Method for Manufacturing Carbonyl Difluoride*, Japan Patent 267,712 (2003).

Morsi, S. A. and Alexander, A. J., "An Investigation of Particle Trajectories in Two-Phase Flow Systems," *J. Fluid Mech.*, **55**(2), 193 (1972).

Perry, R. H., Green, D. W. and Maloney, J. O., *Perry's Chemical Engineers' Handbook*, McGraw-Hill, 6th edition, New York (1984).

Peskin, R. L., *Turbulent Fluid–Particle Interaction, in: G Hetsronil (Ed.), Handbook of Multiphase System*, Hemisphere Publishing Corporation, Washington DC (1982).

Takashima, M. and Yonezawa, S., *Production of Carbonyl Fluoride*, Japan Patent 116,216 (1999).

Tuzla, K. and Chen, J. C., "Performance of a Cyclone under High Solid Loadings," *AIChE Symp. Ser.*, **88**(289), 130 (1992).

Webster, J. L., *Manufacture of Carbonyl Fluoride*, PCT WO 96/19409 (1996); *Manufacture of Carbonyl Fluoride*, U.S. Patent 5,648,530 (1997); *Process for the Preparation of Perfluorocarbons*, U.S. Patent 5,744,657 (1998).

Xiaodong, L., Jianhua, Y., Yuchun, C., Mingjiang, N. and Kefa, C., "Numerical Simulation of the Effects of Turbulence Intensity and Boundary Layer on Separation Efficiency in a Cyclone Separator," *Chemical Engineering Journal*, **95**, 235 (2003).

Yang, K. W. and Yoshida, H., "Effect of Mist Injection Position on Particle Separation Performance of Cyclone Scrubber," *Separation and Purification Technology*, in press (2004).